

# Quantum Polar Metric Learning: Efficient Classically Learned Quantum Embeddings

VINAYAK SHARMA, School of Computing and Augmented Intelligence, Arizona State University, USA

AVIRAL SHRIVASTAVA, School of Computing and Augmented Intelligence, Arizona State University, USA

Deep metric learning has recently shown extremely promising results in the classical data domain, creating well-separated feature spaces. This idea was also adapted to quantum computers via *Quantum Metric Learning* (QMeL). QMeL consists of a 2 step process with a classical model to compress the data to fit into the limited number of qubits, then train a *Parameterized Quantum Circuit* (PQC) to create better separation in Hilbert Space. However, on *Noisy Intermediate Scale Quantum* (NISQ) devices. QMeL solutions result in high circuit width and depth, both of which limit scalability. We propose Quantum Polar Metric Learning (*QPMEL*) that uses a classical model to learn the parameters of the polar form of a qubit. We then utilize a shallow PQC with  $R_y$  and  $R_z$  gates to create the state and a trainable layer of  $ZZ(\theta)$ -gates to learn entanglement. The circuit also computes fidelity via a SWAP Test for our proposed Fidelity Triplet Loss function, used to train both classical and quantum components. When compared to QMeL approaches, *QPMEL* achieves 3X better multi-class separation, while using only 1/2 the number of gates and depth. We also demonstrate that *QPMEL* outperforms classical networks with similar configurations, presenting a promising avenue for future research on fully classical models with quantum loss functions.

CCS Concepts: • **Computing methodologies** → **Dimensionality reduction and manifold learning**; • **Hardware** → **Quantum computation**.

Additional Key Words and Phrases: Metric Learning, Quantum Computing, Quantum Machine Learning, Triplet Loss

## ACM Reference Format:

Vinayak Sharma and Aviral Shrivastava. 2024. Quantum Polar Metric Learning: Efficient Classically Learned Quantum Embeddings. 1, 1 (January 2024), 12 pages. <https://doi.org/10.1145/nnnnnnnn.nnnnnnnn>

## 1 INTRODUCTION

In 2017, Biamonte et al [2] showed that the ability of Quantum Computers to produce *atypical patterns* which are hard to produce classically, gives them a distinct advantage in the domain of machine learning. However, most devices today are considered *Noisy Intermediate Scale Quantum* (NISQ) devices, which are limited in the circuit breadth (number of qubits) and suffer from high noise at larger circuit depths. Due to this, recent works have focused on creating *Quantum Machine Learning* (QML) models that can be run on NISQ devices.

The main challenge in QML remains to define an efficient mapping  $x \in \mathbb{R}^n \rightarrow |\phi(x)\rangle$  that encodes the classical data into the Hilbert Space. Traditional methods that utilize handcrafted schemes such as Angle encoding are space-inefficient

---

Authors' addresses: Vinayak Sharma, vsharm87@asu.edu, School of Computing and Augmented Intelligence, Arizona State University, P.O. Box 878809, Tempe, Arizona, USA, 85287-8809; Aviral Shrivastava, Aviral.Shrivastava@asu.edu, School of Computing and Augmented Intelligence, Arizona State University, P.O. Box 878809, Tempe, Arizona, USA, 85287-8809.

---

Permission to make digital or hard copies of all or part of this work for personal or classroom use is granted without fee provided that copies are not made or distributed for profit or commercial advantage and that copies bear this notice and the full citation on the first page. Copyrights for components of this work owned by others than ACM must be honored. Abstracting with credit is permitted. To copy otherwise, or republish, to post on servers or to redistribute to lists, requires prior specific permission and/or a fee. Request permissions from [permissions@acm.org](mailto:permissions@acm.org).

© 2024 Association for Computing Machinery.

Manuscript submitted to ACM

Manuscript submitted to ACM

1

( $n$  values require  $n$  qubits) or require complex circuits. Most critically, all of these schemes demonstrate poor utilization of the Hilbert Space as shown by Lloyd et al[8].

Quantum Metric Learning (QMeL)[8] was proposed to address both issues by first compressing the data via a classical method (normally a linear layer) and then using a PQC to learn a mapping that maximizes the separation of the embeddings. This 2-step process is inefficient in the number of operations (gates) performed on the qubits, which for NISQ devices can lead to high noise and errors. Additionally, the larger number of gates also leads to overfitting.

In order to address these 2 challenges, we propose Quantum Polar Metric Learning (*QPMeL*) – a novel method that uses a classical model to learn the parameters of the polar form of a qubit. *QPMeL* creates a more efficient mapping that uses shallower circuits while improving multi-class separability in Hilbert Space.

However, learning the polar form of a qubit classically has 2 main challenges:

- (1) Classical distance metrics (such as Euclidean Distance) are not well suited to the curved Hilbert Space. These metrics were formulated for flat feature spaces.
- (2) Encoding classical values via a single  $\sigma$ -gate does not sufficiently capture the 3-D nature of a qubit (in the polar representation) as rotation about a single axis is limited to covering a 2D slice.

*QPMeL* addresses these challenges with the following contributions:

- (1) A novel classical network that encodes classical data into 2 real-valued vectors that are used as Polar coordinates of a qubit. This allows us to utilize the entire 3D space of a qubit, as we are not limited to a single plane.
- (2) A hybrid Hilbert space distance metric we dub "*Fidelity Triplet Loss*" that measures distance in Hilbert Space while creating the optimization target classically. The distances are measured in-circuit while their difference is computed classically.
- (3) *Quantum Residual Corrections* to speed up model learning and generate more stable gradients by acting as a noise barrier. The parameters absorb noisier gradients to allow the classical model to learn more efficiently.

We find that *QPMeL* outperforms the previous QMeL method both in capability and computational complexity. We achieve a high degree of separation between all 10 classes using only 3 qubits and 4 gates per qubit. This is a 3x reduction compared to the 2-layer QAOA implementation of [8]. We also demonstrate that *QPMeL* outperforms classical networks with similar structures to our classical head, presenting a promising avenue for future research on fully classical models with quantum loss functions.

## 2 BACKGROUND

As highlighted in Section. 1, one of the limiting challenges in QML is an efficient mapping of classical data to the Hilbert Space. Traditionally, this mapping used handcrafted circuits such as *Basis State Encoding*, *Amplitude Encoding* and *Angle Encoding*. However, basis and angle encoding do not scale with larger data sizes on NISQ devices. While amplitude encoding has exponential scaling (i.e.  $n$  qubit can encode  $2^n$  values), it requires normalization constraints as well as complex ansatz searches.

### 2.1 Quantum Feature Space

Unlike classical machine learning where the Feature space is normally characterized by a feature vector  $x \in X$ , where  $x \in \mathbb{R}$ , the feature space for *Quantum States* is the *Hilbert Space* ( $\mathcal{H}$ ). This complex vector space is parameterized by the amplitudes of our qubits. The advantage of a Hilbert Space  $\mathcal{H}$  is the exponential size, which allows Quantum Computers to efficiently process information and achieve dramatic speedups over classical computers. Additionally, as

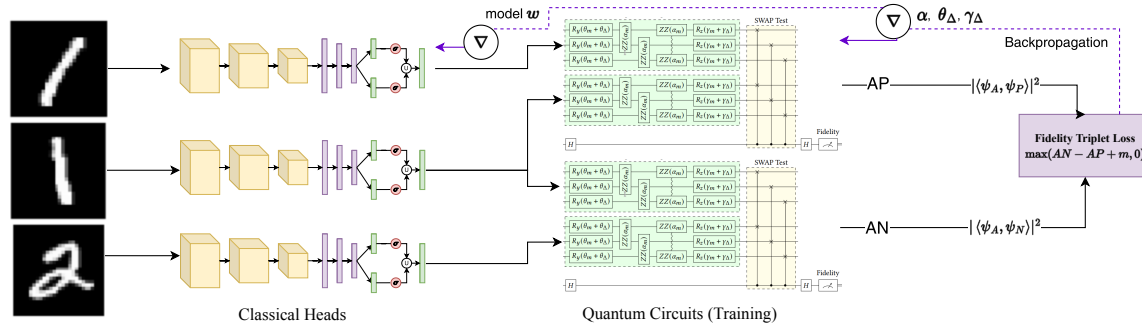


Fig. 1. *QPMel* triplet training loop. The fidelity triplet loss is computed based on the SWAP test fidelity measurement and the gradients are backpropagated throughout. The classical model weights, ZZ parameters and QRC parameters are updated together, having the classical head directly learn the polar coordinates that create separation in Hilbert Space.

$\mathcal{H}$  is complex, it is naturally higher dimensional than any  $x \in \mathbb{R}$  that it encodes, allowing for natural kernel methods to be applied to it. Both of these ideas are explored in Havlíček et al. [4]. However, as demonstrated in Sierra-Sosa et al. [12], the effectiveness of these methods is highly sensitive to the initial state preparation or encoding.

The 3 most common methods for encoding classical data into quantum states are *Basis Encoding*, *Amplitude Encoding*, and *Angle Encoding*. While these are the most common, more specialized encoding schemes have been proposed, and some of those most relevant in *Quantum Machine Learning*(QML) are outlined in Schuld and Petruccione [11].

**2.1.1 Learned Encoding Schemes.** A proposed solution to this problem was in the form of *Learned Encoding Schemes* for QML tasks. In this paradigm, a classical computer learns a lower dimensional representation of the data via methods such as PCA or Deep Neural Networks(DNNs) and these are then used as the input to a QML circuit. However, as shown by Lloyd et al [8], the main challenge with this approach is the poor utilization of the Hilbert Space as the classical model creates real-valued nonperiodic bottlenecks that do not translate well to the complex, exponential and periodic natural of Hilbert Space.

**2.1.2 Quantum Metric Learning (QMeL).** In order to create embeddings that better utilize the Hilbert space, [8] proposed a 2-step procedure of first learning a compressed classical representation and the training a "*Hybrid Bottleneck*" consisting of a PQC (They used the QAOA scheme) and a single classical dense layer to learn better separation. The approach utilized Hilbert Space distance metrics such as *State Fidelity*, *Helström* or *Hilbert-Schmidt* to implement a procedure similar to Deep Metric Learning.

**2.1.3 Fidelity.** is the measure of closeness between two quantum states and can be computed both analytically or via a "*SWAP Test*" circuit. We can define the fidelity between 2 states  $\rho, \psi$  as :

$$F(\rho, \psi) = |\langle \rho | \psi \rangle|^2 \quad (1)$$

This is analogous to the cosine similarity metric used in classical metric learning as the inner product between states measures a similar notion of similarity.

### 3 RELATED WORK

The idea of Quantum Metric Learning (QMeL) was first proposed by Lloyd et al. [8]. They suggested first training a classical classifier to serve as a feature extractor. The classifier is then frozen and the classification head is replaced with a linear layer. This layer creates the bottleneck that is then embedded into a Quantum Computer via the QAOA embedding scheme. The linear layer and QAOA layers are then jointly trained to optimize the *State Overlap* that was measured via the Hilbert Schmidt Distance. However, the authors noted that the method suffered from overfitting issues due to the depth of the circuit.

Schuld [10] later extended this interpretation into the study of *kernel methods*. Schuld argues that the mapping onto Hilbert Space can be equated to *Classical Kernel methods* that are executed on a quantum computer. This interpretation implies that all the computation is largely dependent on the encoding as the embedding would fix the kernel. The task of encoding can then be defined as learning the function  $\phi$  such that  $x \rightarrow |\phi(x)\rangle$  can map the classical data to the Hilbert Space. This method was then extended by Jerbi et al. [6], to create the *data re-uploading circuit*. Data re-uploading circuits proved that even single qubit circuits can be universal function approximators, a result that contradicts the kernel-model paradigm as a single classical data point does not correspond to a single quantum state (or a single mapping).

While all of these methods showed large improvements, they all required much deeper circuits and had issues with overfitting. Additionally, [8] was only demonstrated on binary classes and [6, 10] both faced scaling problems when looking at multiple classes.

Hou et. al. [5], were the first to propose an adversarial metric method based on the aforementioned Triplet Loss. They introduced the idea of computing the triplet loss in the circuit as an optimization step. However, a key limitation was that they also only focused on binary classification. *QPMeL* extends this idea to multiple classes while splitting the Triplet loss computation into a distance and loss step computed in and out of the circuit respectively.

Recently, Liu et al. [7], introduced the idea of *Quantum Few Shot Learning* alongside the *Circuit Bypass Problem* (CBP). Of key interest to this work is the CBP as it allows for a possible method to classically learn efficient quantum mappings. In their paper, the authors define CBP as the tendency of the classical parameters of Hybrid Neural Networks (HyNNs) to learn optimized representations of the dataset without large differences from the Quantum kernel. The proposed cause is that the classical network treats the circuit as a strange non-linearity and optimizes only to get the correct results from the circuit while ignoring its utilization. *QPMeL* aims to exploit this property to produce more stable and efficient embeddings using Triplet Loss in Hilbert Space.

While [5] recently also proposed a quantum version of triplet loss, they were more focused on the adversarial properties of the loss function and calculated it entirely in-circuit via amplitudes encoding and interference. Additionally, they were limited to  $R_y$  rotations.

### 4 PROPOSED METHOD

The core of *QPMeL* is splitting the learning process between a classical and quantum component as is standard with HyNNs but moving the majority of the learnable parameters to the classical components. We accomplish this by learning the parameters of the polar qubit representation as independent network outputs. *QPMeL* is an extension of the work by [7] and [8] and has 4 main components:

- (1) **Classical Head:** formed by our CNN Backbone and "*Angle Prediction Layer*",
- (2) **Quantum Circuits:** Which encodes the classical data and performs the fidelity measurement.

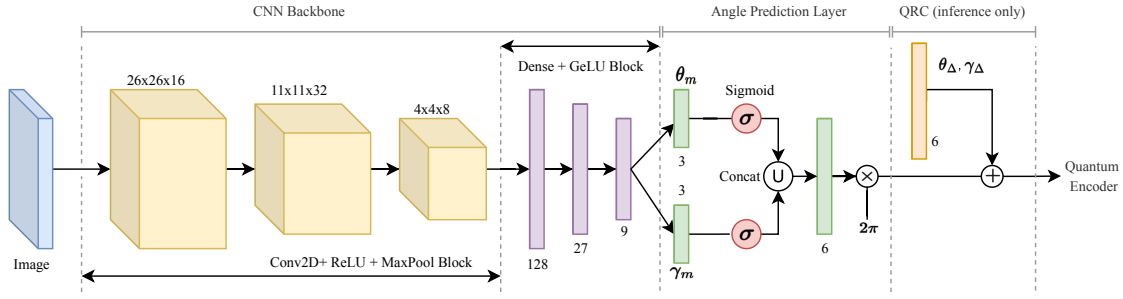


Fig. 2. *QPMEL* Classical Head Architecture. Our angle prediction layer learns independent  $\theta$  and  $\gamma$  from the features of the CNN Backbone. The sigmoid activation and  $2\pi$  multiplication are used to match the period of rotation in a qubit. Quantum Residual Correction is then applied for inference.

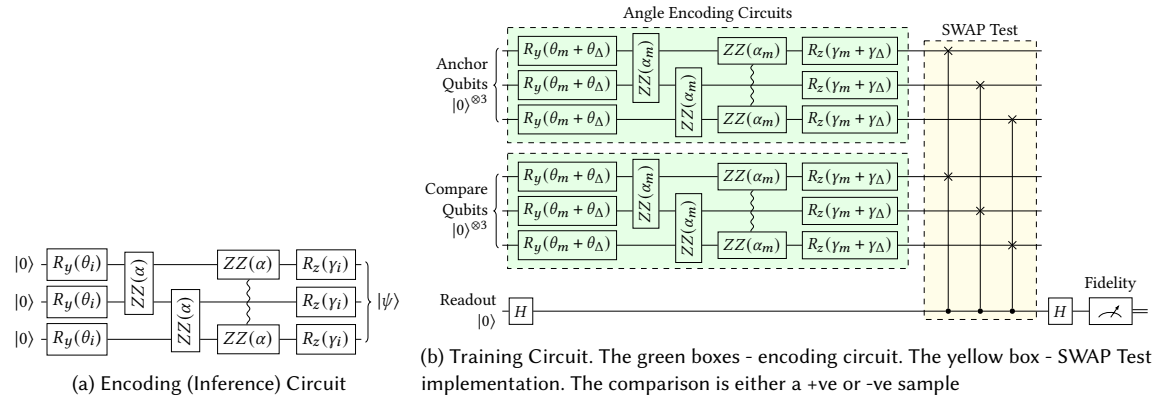


Fig. 3. Our Quantum Circuits for training and inference. The QRC parameters are learned as separate weights during training, acting as noise barriers to the classical head. During inference, the parameters are integrated into the classical head.

- (3) **QRC**: An extension to our training circuit that leads to faster training via an additive freely trainable parameter.
- (4) **Loss Function**: Finally, our loss function is a novel adaptation of the Triplet Loss function to the Hilbert Space. We call this the "*Fidelity Triplet Loss*".

#### 4.1 Classical Head

**4.1.1 CNN Backbone.** The classical head uses convolution blocks consisting of CONV + ReLU + MaxPool layers, a dense block with 3 Dense + GeLU layers with reducing dimensionality. GeLU has better convergence properties in Dense layers and hence is chosen over ReLU. The architecture can be seen in 2.

**4.1.2 Angle Prediction Layer (APL).** The polar form of a qubit can be described in terms of 2 angles -  $\theta$  and  $\gamma$  which can be encoded via the  $R_y$  and  $R_z$  gates respectively. Due to the rotational nature of these gates, any encoding method using them is periodic. As pointed out in [8], when trained together, the classical ReLU learned this periodic property. However, we argue that encoding values directly within the range of the period via a sigmoid and multiply procedure is more efficient.

*QPMeL* aims to learn "Rotational Representations" for classical data by creating 2 embeddings for the  $\theta$  and  $\gamma$  parameters respectively per qubit from the classical head. Therefore for a 3 qubit embedding our classical model would output 6 real values. We ensure that these values are within the period by utilizing the sigmoid activation and multiplying the results by  $2\pi$  before passing them to the circuit. This explicit period definition ensures more stable losses as we do not need to worry about overlapping values with similar gradients. The idea of rotational embeddings has also been noted in classical networks by Zhou et al[13], where they demonstrated that rotational representations have continuous representations in 5D and 6D, which lend themselves well to be learned by neural networks. We can hence define the angle prediction layer as follows:

$$\begin{aligned} x &= \text{CNN\_Backbone}(\text{Image}) \\ \theta_m &= \text{sigmoid}(W_\theta x + b_\theta) \quad | \quad \gamma_m = \text{sigmoid}(W_\gamma x + b_\gamma) \\ \text{APL} &= 2\pi \times \text{concat}(\theta_m, \gamma_m) \end{aligned}$$

Where,  $W_\theta, b_\theta$  are the weights and bias for the  $\theta$  prediction layer and  $W_\gamma, b_\gamma$  are the weights and bias for the  $\gamma$  prediction layer.

## 4.2 Quantum Circuits

**4.2.1 Encoding Circuit.** The encoding circuit is used to create the state  $|\psi\rangle$  from the classical embeddings. The structure (as shown in Fig3a) consists of  $R_y$  and  $R_z$  gates separated by a layer of cyclic  $ZZ(\theta)$  gates for entanglement. Our experiments show that this structure performs similarly to or slightly better than an  $R_y \rightarrow R_z \rightarrow ZZ$  structure which more naturally shows polar learning. The choice of  $ZZ(\theta)$  is motivated by the variable entanglement property as also observed by [8].

**4.2.2 Embedding State and Learnable Parameters.** The final state produced by our Encoding circuit as seen in Fig 3a would be:

$$|\psi\rangle = \bigotimes_{i=0}^n \exp(i\frac{\phi_i}{2}) \cos\frac{\theta_i}{2} |0\rangle + \exp(i\frac{-\phi_i}{2}) \sin\frac{\theta_i}{2} |1\rangle \quad (2)$$

where,

$$\begin{aligned} \phi_i &= \alpha_k - \alpha_i - \gamma_i \\ k &= (n + i) \quad \text{mod} \quad (n + 1) \\ \theta_i &= \theta_{m_i} + \theta_{\Delta_i} \quad | \quad \gamma_i = \gamma_{m_i} + \gamma_{\Delta_i} \\ \theta_{m_i}, \gamma_{m_i} &= f(\text{image}, w) \end{aligned}$$

Where we have 6 parameters per qubit, 2 from the classical model ( $\theta_m, \gamma_m$ ), 2 learned parameters for the  $ZZ$ -Gate ( $\alpha_i, \alpha_k$ ) and 2 residuals ( $\theta_{\Delta}, \gamma_{\Delta}$ ).

**4.2.3 Training Circuit.** *QPMeL* uses separate circuits for training and inference, with 2 main differences - (1). The SWAP test extension requires 2 copies of the encoding circuit (2). Residual Corrections that are only used in the training process. We can see the green regions in Fig 3b use our encoding circuit but add the QRC parameters ( $\theta_{\Delta}, \gamma_{\Delta}$ ) to the rotations.

In order to compute the fidelity we use the SWAP test. We measure  $M = P(|0\rangle)$  and convert it to fidelity classically using the formula:

$$F = 2M - 1$$

This structure is seen in the yellow regions alongside the readout qubit on the bottom.

### 4.3 Quantum Residual Corrections (QRC)

We introduce the idea of QRC to speed up the training process and mitigate the smaller gradients that we get due to *Sigmoid Saturation*[3] impacting the early layers of our classical model alongside the smaller gradients from our quantum circuit. While using GeLU and ReLU throughout our classical model mitigates the issue of *Sigmoid Saturation*[3], it is the combination of the 2 that creates the issue. Quantum gradients are approximated using the *parameter-shift rule* [9], which utilizes periodic properties of the gates to calculate the gradients, but this also leads to smaller gradients.

To overcome this issue we propose a novel new method we name "QRC". We add learnable parameters  $\theta_\Delta$  and  $\gamma_\Delta$  to the angles of the  $R_y$  and  $R_z$  gates respectively as seen in Fig.3. Due to their shallowness and input independence, they are affected by smaller gradients faster and act as "noise barrier" allowing our classical to learn faster. During inference, we add these weights to our classical model as seen in Fig 2

### 4.4 Fidelity Triplet Loss

*QPMEL* uses a quantum extension to triplet loss, which uses *State Fidelity* as the distance metric. We simplify our loss function by separating the comparison and distance formulation, favoring 2 calls to a much thinner and shallower circuit as compared to [5]. This is more practical on NISQ devices with lower coherence time. *QPMEL* measures distances in Hilbert space using state fidelity and then computes the difference classically. The final loss function in *QPMEL* can be defined as follows:

$$AP = |\langle \psi_A | \psi_P \rangle|^2 \quad | \quad AN = |\langle \psi_A | \psi_N \rangle|^2$$

$$Loss = \max(AN - AP + m, 0)$$

Where  $\psi_A, \psi_P, \psi_N$  are the quantum states of the Anchor, Positive and Negative samples respectively.  $m$  is the margin hyperparameter.

A key difference from the classical counterpart is using  $AN - AP$  rather than  $AP - AN$ . This is a natural result of the difference between Fidelity and MSE distance metrics. The classical formulation tries to minimize AP Distance, as  $MSE(A, P) \rightarrow 0$  for similar features. However, in the quantum case, we try to maximize the fidelity, as  $F(\psi_A, \psi_P) \rightarrow 1$  for similar states.

## 5 EXPERIMENTAL SET-UP

All experiments were carried out using the 'lightning.qubit' and 'default.tf' backends on pennylane for our quantum simulations. The MNIST dataset was used as a benchmark with testing using the test set defined in the tf.dataset version, not seen by any models during training. We use the "All Pair Distances" for visualization which are plotted as heatmaps. We randomly take 1000 samples for each ordered pair, the results of which are averaged to create the heatmaps. We use a margin( $m$ ) of 0.9 for all experiments (both MSE and Fidelity)

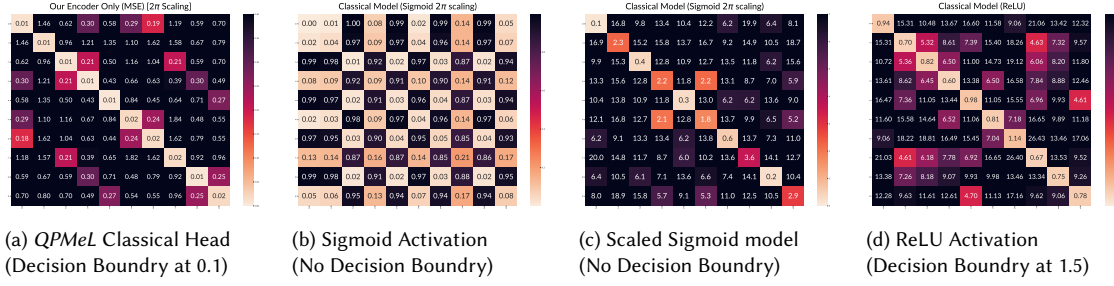


Fig. 4. All Pair heatmaps in Euclidean space: (a) and (c) have the same model architecture but show large differences in separability. (b) shows perfect separability but via an unbounded upper limit as seen by the magnitude of values.

**5.0.1 MinMax Metric:** We propose the "MinMax" metric to quantify our embedding performance. The metric is feature space agnostic as it directly operates on the pre-computed distances using the native space distance metric (MSE or fidelity). However, as the metric trends are reversed for MSE and Fidelity, we present the results separately and use  $1 - \text{distances}$  for Fidelity. The metric computes the distance of the  $AP_{max}$  and  $AN_{min}$ , which corresponds to the worst case for both and represents it as a %  $AN_{min}$ . These are computed on the averages seen in the heatmap to avoid outliers.

Positive values indicate that we can draw a decision boundary between the classes while negative values indicate that the classes are not separable with this feature space. Additionally, the magnitude of the value indicates the degree of separation.

Diff (Higher is Better)				
Model	$AP_{max}$	$AN_{min}$	Diff	% of $AN_{min}$
<i>QPMeL</i> Model	0.075	0.906	0.831	91.681
No Residual Model	0.092	0.051	-0.041	-81.363
QMeL[8] Model	0.489	0.018	-0.470	-2579.563
QMeL+ Model	0.363	0.483	0.120	24.882

Table 1. MinMax Metric for Hilbert Space: We can see that both the original and the no residual models cannot create a decision boundary, our model

## 6 EMPIRICAL RESULTS AND OBSERVATIONS

**6.0.1 Classical Baselines:** We trained 3 models with the same structure as our classical model in Fig.2 but different activations on the final layer - (1). **Sigmoid Model** with sigmoid activation, (2). **Scaled Sigmoid model** adds  $2\pi$  scaling to (1) and (3). **ReLU model** with ReLU activation. All were trained with MSE Triplet Loss. We compare them against the Classical Head before applying QRC (till  $2\pi$  multiplication in Fig.2).

**6.0.2 Quantum Baselines:** We establish 3 Quantum Baselines - (1). **No Residual Model** which is identical to *QPMeL* but without QRC, (2). **QMeL[8]** a lightly modified version of the original using our Fidelity triplet loss and (3). **QMeL+**, a heavily modified version of the original using MSE Triplet Loss for pre-training alongside our Fidelity Triplet Loss.



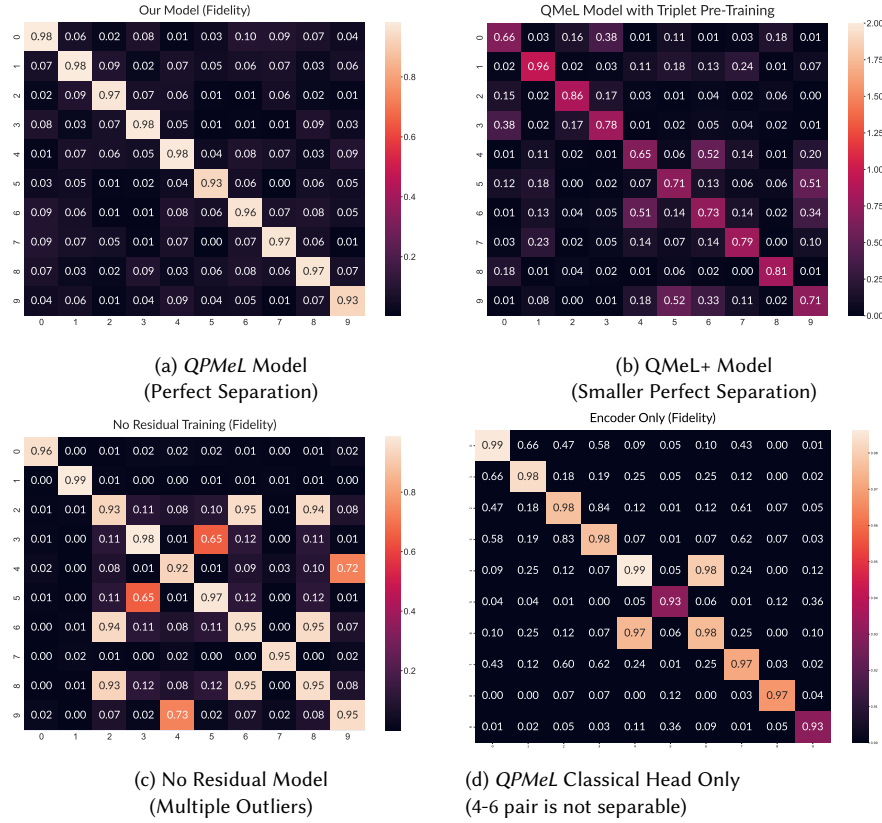


Fig. 5. All Pair heatmaps in Hilbert Space: (a) shows our model fully trained with residuals, with perfect separation and large differences. (b). shows the same model trained without residuals with multiple outliers. (c). only creates binary separation for the digit 9 (d). shows a modified version of the *QMeL* model with perfect separation but smaller differences between +ve and -ve classes.

### 6.1 3x better separation using 1/2 the number of gates and circuit depth compared to *QMeL*

The original *QMeL* framework [8] as explained in Sec. 3 used an overlap loss that did not scale well to multi-class tasks. The modified version with our Fidelity Triplet Loss also failed to create a decision boundary as seen in Table.1 where it produces a -ve difference. When we apply a more robust separation method for the pre-quantum step (*QMeL+*) the difference in Table.1 is +ve implying that a decision boundary can be made but the magnitude is only 24% of  $AN_{min}$  implying that the clusters are close together.

In contrast, *QPMeL* produces a +ve difference that is 91% of  $AN_{min}$ , showing 3x improvement over *QMeL+*. We see this trend reflected in Fig.5a and Fig.5b with the difference in magnitude between the diagonal and everywhere else. Additionally, looking at the parameters in Table 2 *QPMeL* utilizing 1/2 (9 vs 21) the number of gates, 1/2 (5 vs 11) the circuit depth and (11k vs 16k)20% fewer classical parameters compared to *QMeL/QMeL+*

Model	# of Gates	Circuit Depth	Classical Parameters
QMeL/QMeL+	21	11	16,645
<i>QPMeL</i> Model	9	5	11,099

Table 2. Computation complexity comparison: Our model uses (1/2) the number of gates and (1/2) the circuit depth and 50% fewer classical parameters compared QMeL with better performance.

## 6.2 Quantum loss functions may improve the learning of classical models

Look at Table 3, both sigmoid models produce -ve differences which indicate the absence of a decision boundary. The *QPMeL* classical head has an identical structure to the **Scaled Sigmoid model** with only a difference in the loss function. However, it produces a +ve difference of 88% of  $AN_{min}$ , implying that a strong decision boundary exists.

As both models are capable of learning the same family of functions due to identical model architectures, the difference is indicative that our quantum loss function allows the classical head to learn a better metric function. Additionally, the *QPMeL* classical head also shows an 18% improvement over the ReLU model (Table 3), proving that the improvement is substantial. As noted by [7] in their CBP, the classical network treats our circuit as an unknown non-linearity which we argue is benefiting the learning capability of the classical head. We believe that this is a promising avenue for future research, which can be explored further by using the *QPMeL* framework for other classical tasks.

## 6.3 *QPMeL* strongly Couples Euclidean and Hilbert embedding seperation

Despite never being trained on any Euclidean loss function such as MSE-Triplet Loss, the *QPMeL* classical head produces a strong separation between classes as seen by the 88% of  $AN_{min}$  in Table 3. We can also see in Fig 4a that this separation is well distributed across all pairs.

This is because, as is clear from Eqn 2, the state produced by the encoding circuit is directly dependent on the classical model outputs of  $\theta, \gamma$ . Therefore to learn separability in Hilbert Space, our loss function enforces separation in Euclidean Space due to the no overlap guarantee of the  $2\pi$  output scaling.

## 6.4 QRC enables the classical head to learn decision boundaries in Hilbert Space

From the results in Table. 1, we can see that the No Residual model fails to learn a clear decision boundary. However, looking Fig 5c, while the model fails to create a decision boundary, the issues are localized to specific pairs (ex. (8,2)), while all other regions remain well separated. We believe this is due to smaller gradients which require more training time and data to learn these corner cases. However, PQCs are known to have barren plateaus which can make training unstable.

In contrast, our model can learn a decision boundary for all classes. Fig 5d, shows that even before applying our corrections the encoder struggles with a single pair. This implies that QRC is helping the classical model learn the corner cases faster. This is further supported by the fact that the QRC is only used during training and not during inference. This hints that the residual framework eases the task on the classical head allowing it to learn faster and more robustly.

## 7 DISCUSSION

While the power of Hilbert Space when utilizing PQC has been well explored [1], their effectiveness as a non-linear feature space for classical optimization with DNN is still an open question.

Diff (Higher is Better)				
Model	$AP_{max}$	$AN_{min}$	Diff	% of $AN_{min}$
<i>QPMeL</i> Model	0.141	1.143	1.002	87.685
<i>QPMeL</i> Classical Head	0.003	0.029	0.026	88.303
ReLU Model	1.161	4.605	3.445	74.800
Sigmoid Model	0.193	0.012	-0.181	-1474.017
Scaled Sigmoid Model	3.644	1.935	-1.709	-88.331

Table 3. MinMax Metric, Euclidean Space: Sigmoid models cannot create decision boundaries. The remaining models create a decision boundary. *QPMeL* models perform the best

A major advantage of this approach is that it naturally factorizes the  $2^n$  complex-valued Hilbert Spaces using  $n$  real values. However, it is important to understand that a single angle is not sufficient to represent a qubit as it only represents a rotation about a single axis. This would limit our network to points within a single 2D slice of the Hilbert Space. However, 3 rotational angles would not be required as the normality constraint of the qubit would limit the 3rd angle to be a function of the other 2. Therefore, our "*Angle Prediction Layer*" consists of 2 sets of angles -  $\theta$  (the  $R_y$  parameter) and  $\gamma$  (the  $R_z$  parameter). To learn these angles, we use a single dense layer with the number of units equal to the number of qubits.

## 8 CONCLUSION

PQCs and QML as an extension present a promising new avenue for research. However, the limitation of current hardware makes near-term applications difficult to realize. In this paper, we propose the *QPMeL* framework that learns the polar representation of qubits via Hilbert Space Metric Learning. We also introduce the idea of QRC which helps alleviate the issues of sigmoid saturation[3] and barren plateaus. Our results present a promising new direction for research utilizing PQCs as loss functions or non-linear activations to enhance classical models and show strong representation learning.

## REFERENCES

- [1] Amira Abbas, David Sutter, Christa Zoufal, Aurélien Lucchi, Alessio Figalli, and Stefan Woerner. 2021. The power of quantum neural networks. *Nature Computational Science* 1, 6 (2021), 403–409.
- [2] Jacob Biamonte, Peter Wittek, Nicola Pancotti, Patrick Rebentrost, Nathan Wiebe, and Seth Lloyd. 2017. Quantum machine learning. *Nature* 549, 7671 (2017), 195–202.
- [3] Bin Ding, Huimin Qian, and Jun Zhou. 2018. Activation functions and their characteristics in deep neural networks. In *2018 Chinese Control And Decision Conference (CCDC)*. 1836–1841. <https://doi.org/10.1109/CCDC.2018.8407425>
- [4] Vojtěch Havlíček, Antonio D. Córcoles, Kristan Temme, Aram W. Harrow, Abhinav Kandala, Jerry M. Chow, and Jay M. Gambetta. 2019. Supervised learning with quantum-enhanced feature spaces. *Nature* 567, 7747 (mar 2019), 209–212. <https://doi.org/10.1038/s41586-019-0980-2>
- [5] Yan-Yan Hou, Jian Li, Xiu-Bo Chen, and Chong-Qiang Ye. 2023. Quantum adversarial metric learning model based on triplet loss function. arXiv:2303.08293 [quant-ph]
- [6] Sofiene Jerbi, Lukas J. Fiderer, Hendrik Poulsen Nautrup, Jonas M. Kübler, Hans J. Briegel, and Vedran Dunjko. 2023. Quantum machine learning beyond kernel methods. *Nature Communications* 14, 1 (jan 2023). <https://doi.org/10.1038/s41467-023-36159-y>
- [7] Minzhao Liu, Junyu Liu, Rui Liu, Henry Makhanov, Danylo Lykov, Anuj Apte, and Yuri Alexeev. 2022. Embedding Learning in Hybrid Quantum-Classical Neural Networks. In *2022 IEEE International Conference on Quantum Computing and Engineering (QCE)*. IEEE. <https://doi.org/10.1109/qce53715.2022.00026>
- [8] Seth Lloyd, Maria Schuld, Aroosa Ijaz, Josh Izaac, and Nathan Killoran. 2020. Quantum embeddings for machine learning. arXiv:2001.03622 [quant-ph]
- [9] K. Mitarai, M. Negoro, M. Kitagawa, and K. Fujii. 2018. Quantum circuit learning. *Physical Review A* 98, 3 (Sept. 2018). <https://doi.org/10.1103/physreva.98.032309>
- [10] Maria Schuld. 2021. Supervised quantum machine learning models are kernel methods. arXiv:2101.11020 [quant-ph]

- [11] Maria Schuld and Francesco Petruccione. 2018. *Supervised learning with quantum computers*. Vol. 17. Springer.
- [12] Daniel Sierra-Sosa, Michael Telahun, and Adel Elmaghraby. 2020. TensorFlow Quantum: Impacts of Quantum State Preparation on Quantum Machine Learning Performance. *IEEE Access* 8 (2020), 215246–215255. <https://doi.org/10.1109/ACCESS.2020.3040798>
- [13] Yi Zhou, Connelly Barnes, Jingwan Lu, Jimei Yang, and Hao Li. 2020. On the Continuity of Rotation Representations in Neural Networks. arXiv:1812.07035 [cs.LG]